Quantum Electronics **49** (10) 919–924 (2019)

https://doi.org/10.1070/QEL17053

All-fibre single-mode small-signal amplifier operating near 0.976 μm

S.S. Aleshkina, D.S. Lipatov, T.A. Kochergina, V.V. Velmiskin, V.L. Temyanko, L.V. Kotov, T.L. Bardina, M.M. Bubnov, A.N. Guryanov, M.E. Likhachev

Abstract. **We have developed and demonstrated a polarisation-maintaining single-mode ytterbium-doped fibre for light amplification at a wavelength near 0.976 μm in an all-fibre configuration. A distinctive feature of the proposed fibre design is low losses due to fusion splices with standard single-mode fibre having a core diameter of 10 μm, which has made it possible to produce an all-fibre small-signal amplifier with a gain threshold near 3 W and a differential pump-to-signal conversion efficiency of 9.8% in the saturation regime. The proposed amplifier has been shown to be well-suited for small-signal amplification. In particular, at an input signal power near 1 mW and a gain of 20 dB, the ratio of the amplified signal to the integrated luminescence intensity near 0.976 μm exceeds 20 dB. A 40-dB gain has been demonstrated for an ultrasmall signal of ~10-μW power.**

Keywords: *ytterbium-doped optical fibre, large mode area fibre, ytterbium fibre amplifier.*

1. Introduction

Recent years have seen increasing interest in Yb-doped fibre lasers emitting in a spectral range near 0.98 μm, because they are potentially attractive for medical applications (this wavelength corresponds to an absorption peak of water) and for replacing commercially available bulky gas (argon and krypton excimer) lasers via frequency doubling and quadrupling. Most of the research aimed at producing Yb-doped fibre lasers emitting at a wavelength $\lambda = 0.98$ μm has focused on highly efficient, high-average power cw laser sources [1–4]. Note that, for lack of high-power single-mode pump sources [the power of commercially available single-mode laser diodes (LDs) emitting at 0.915 μm does not exceed 300 mW], all configurations and active fibres for the lasing and amplification at a wavelength near 0.976 μm are adapted to pump propagation through the cladding [1–6]. Moreover, pump-to-signal conversion efficiency in lasers and amplifiers operating near $\lambda = 0.976$ μm is limited by the amplification of the spontaneous luminescence of Yb ions in a spectral range near 1.03 μm. This can usually be obviated by reducing the length of the active fibre (at the highest population inversion, the gain coefficient near 0.976 μm is several times that at $\lambda =$ 1.03 μm) and raising the rate of pump absorption from the cladding through an increase in the core to cladding diameter ratio. As a result, the existing active fibre designs are unsuitable for producing all-fibre laser configurations: the large core size and the necessity of selectively exciting the fundamental mode require that bulk optics be used, which compromises the integrity of the laser design and cancels out the advantages of fibre-based configurations (compact design, reliability and low cost) [1–4]. Moreover, even in the case of all-fibre designs [5] the large active-core size leads to high lasing thresholds (tens of watts) and large losses due to fusion splices with standard single-mode fibre, whose core is no more than 10 μm in diameter near 0.976 μm, which is unacceptable for both small-signal amplifiers and all-fibre pulsed master oscillator configurations.

A much more promising approach for producing small-signal amplifiers is to reduce the silica cladding size, but it also has limitations. First, commercially available equipment (fusion splicers, fibre cleavers and other) allows one to deal with fibres whose silica cladding is 80 μm or more in diameter. Besides, reducing the diameter of the silica cladding of an active fibre to below 125 μm rules out the possibility of employing commercially available pump–signal combiners, which are fabricated using double-clad fibre 125 μm in outer diameter.

The objectives of this work were to optimise and fabricate an all-fibre small-signal amplifier operating in a spectral range near 0.976 μm. The ytterbium-doped fibre design was optimised so as to reach high efficiency in the spectral region of interest and ensure low losses due to fusion splices with standard single-mode fibre having a core diameter of 10 μm. To create an all-fibre amplifier configuration, we designed a pump–signal combiner having a signal fibre core size of 10 μm and a silica cladding size of 80 μm. We studied key features of small-signal gain in ytterbium-doped fibre at a wavelength near 0.976 μm.

2. Active fibre design

To numerically model the refractive index profile (RIP) of active fibre, we wrote a program for solving rate equations which took into account the radial mode field intensity distribution and the dopant distribution across the fibre. The fundamental and high order mode field intensity distributions

S.S. Aleshkina, T.A. Kochergina, V.V. Velmiskin, M.M. Bubnov, M.E. Likhachev Fiber Optics Research Center, Russian Academy of Sciences, ul. Vavilova 38, 119333 Moscow, Russia; e-mail: sv_alesh@fo.gpi.ru;
D.S. Lipatov, A.N. Guryanov G.G. Devyatykh Institute of Chemistry of High-Purity Substances, Russian Academy of Sciences, ul. Tropinina 49, 603950 Nizhny Novgorod, Russia;
V.L. Temyanko, L.V. Kotov College of Optical Sciences, University of Arizona, 1630 East University Blvd., Tucson, AZ 85721-0094, USA;
T.L. Bardina Moscow Institute of Physics and Technology (State University), Institutskii per. 9, 141701 Dolgoprudnyi, Moscow region, Russia

Received 29 April 2019
Kvantovaya Elektronika **49** (10) 919–924 (2019)
Translated by O.M. Tsarev

were obtained by solving a scalar wave equation. In our simulations, the fibre was assumed to be axisymmetric.

A major problem with the existing fibre designs for lasing and amplification near 0.976 μm is that they are incapable of ensuring efficient coupling of an amplified signal from their active core to standard passive single-mode fibre, such as is used to fabricate fibre-optic components. For this reason, the active fibre considered here has a core diameter of 10 μm and a core–cladding refractive index difference Δn of 0.002, which ensures single-mode operation of the fibre. We chose a fibre design with a double reflective cladding: one cladding, 80 μm in outer diameter, consisted of undoped silica glass and the other consisted of a low refractive index polymer. The dopant concentration in the core was 10^{26} m^{-3} (0.23 mol%). Varying the ytterbium concentration caused the optimal length of the fibre to vary inversely with it, which had no effect on the fibre operation efficiency at the optimal length. In this study, we simulated a cladding-pumped ($\lambda = 0.915$ μm) amplifier in the copropagating pump and signal configuration. The pump power was taken to be 10 W (sufficient for surpassing the gain threshold) and the input signal power was 0.5 W (operation of the amplifier in the saturation regime). In our simulations, we took into account luminescence copropagating and counterpropagating with the signal.

One way of improving the lasing efficiency of ytterbium-doped fibre near 0.976 μm is by ring-doping a guiding structure [7], while leaving the central part of the core free of Yb^{3+} ions. This allows one to maximise the inversion level of ytterbium ions at a given pump-to-signal power ratio, thus ensuring preferred conditions for light amplification at a wavelength of 0.976 μm. In this study, we assessed the effectiveness of this approach. We examined three types of doping with Yb^{3+} ions (Fig. 1): doping of only the core (configuration I), doping of the core and an adjacent part of the cladding (II) and doping of only a part of the cladding adjacent to the core (with the core remaining undoped) (III). The dopant concentration was the same in all three configurations. Table 1 presents the Yb-doped fibre parameters obtained in our simulations (where I_s is the overlap integral of the mode and the doped region; I_p is the overlap integral of the pump propagation and doped regions; L_{opt} is the optimal length of the active fibre; and η is amplification efficiency). It is seen from Table 1 that the highest fundamental mode amplification efficiency can be reached by doping only the cladding, in which case the overlap integral of the mode field (at the signal and luminescence wavelength) and doped region is minimal, in perfect agreement with previously reported data [7]. At the same time, a distinctive feature of the fibre design under consideration is the reduced diameter of the first reflective cladding and the presence of a second reflective cladding. In this case, an important parameter influencing the mode composition of the amplified signal is the overlap integral of the doped region and high order modes, which are formally under the cutoff wavelength, but propagate in the first reflective cladding due to reflection from the second one. It is known from the literature that, under certain conditions, such modes can be effectively amplified, leading to significant degradation of the output beam quality [8]. It seen from Table 1 that, if only the cladding is doped (Fig. 1, configuration III), the overlap integral of the LP_{11} mode (which is formally under the cutoff wavelength for the first reflective cladding) and ytterbium-doped region exceeds the overlap integral for the LP_{01} fundamental mode, suggesting that the gain coefficient of the LP_{11} mode is larger. It is, therefore, reasonable to expect that ring doping will lead not to an increase in fundamental mode ($\lambda = 0.976$ μm) lasing efficiency but to few-mode signal amplification, which is unacceptable in our case. In connection with this, in this report we examine a fibre design in which both the core and cladding are doped (configuration II).

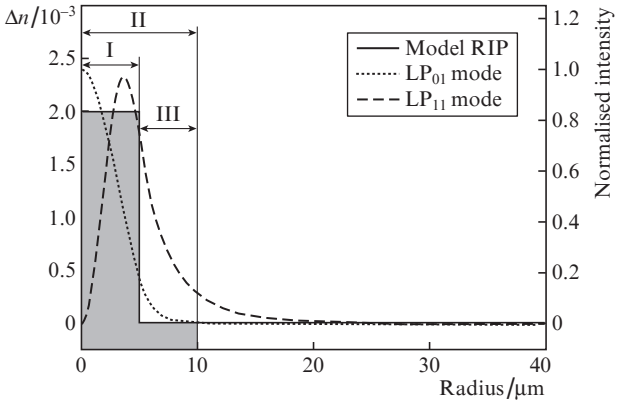

Figure 1. Model refractive index profile of the fibre and LP_{01} and LP_{11} mode field intensity profiles. The doped regions are shown grey: (I) only the core is doped, (II) the core and an adjacent part of the cladding are doped, and (III) only a part of the cladding adjacent to the core is doped.

Table 1. Calculated parameters of the Yb-doped fibre.

Doped region	I_s (LP_{01})	I_s (LP_{11})	I_p	L_{opt}/m	η (%)
I	0.8344	0.3697	0.0156	7	9.5
II	0.9969	0.7993	0.0692	6.5	21.96
III	0.1672	0.4352	0.0538	25	40.39

3. Active fibre design and characteristics

Another problem in designing fibres for lasing near 0.976 μm is the high photodarkening rate, due to the high degree of Yb^{3+} inversion [9]. Because of this, P_2O_5–Al_2O_3–SiO_2 glass was chosen as a doping host insensitive to the photodarkening effect and capable of ensuring high ytterbium ion solubility and a low refractive index of the core [10]. Ytterbium oxide concentration in the glass network was 0.16 mol%. It is worth noting that low sensitivity to the photodarkening effect in phosphoaluminosilicate glass can only be ensured by excess doping with phosphorus oxide [10, 11]. This was done in order to reliably suppress the photodarkening effect. As a result, the refractive index of the region doped with ytterbium ions proved to exceed that of undoped silica. Because of this, the refractive index profile described above was modified so that the core consisted of two ytterbium-doped regions and that the central region had an increased refractive index, which reduced the fundamental mode field diameter.

The fibre preform was produced by the MCVD process. To maintain polarisation, borosilicate rods were inserted in the cladding of the preform. The preform was then drawn into fibre with a silica cladding diameter of 80 μm. During the drawing process, the fibre was coated with a reflective polymer, which ensured a numerical aperture NA ~ 0.45. The refractive index profile of the fibre is presented in Fig. 2. The inset in Fig. 2 shows an image of the fibre end face. It is seen

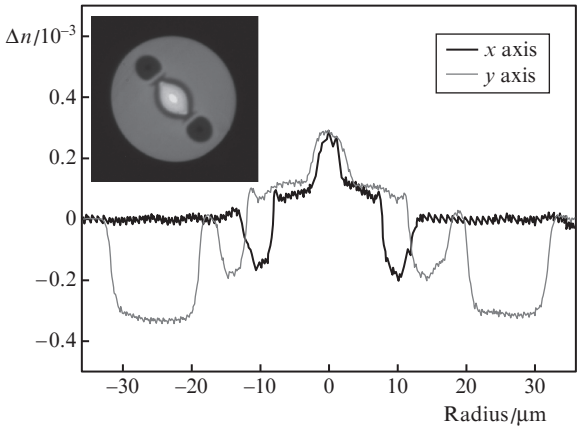

Figure 2. Measured refractive index profiles of the fibre along the x and y axes. Inset: image of the fibre end face.

that the fibre drawing process was accompanied by deformation of the fibre core, which became elliptical.

The mode composition of the fibre core was studied by a beam scanning technique at $\lambda = 1.06$ μm, which was due to the strong absorption by Yb^{3+} ions at a wavelength of 0.976 μm and their spontaneous luminescence near 1.03 μm. Guided modes of the Yb-doped fibre were excited by light delivered through a single-mode step-index fibre with a core diameter of 6 μm, which was translated across the Yb-doped fibre end face. Translating the step-index fibre relative to the test fibre was shown to cause no high order mode excitation (Fig. 3): it only led to a gradual reduction in output beam intensity. This points to single-mode operation of the Yb-doped active fibre at $\lambda = 1.06$ μm. The fundamental mode field diameter along the x and y axes was 12 and 14 μm, respectively. Clearly, the distinction was caused by the ellipticity of the core due to its distortion during the consolidation of the fibre preform with borosilicate rods.

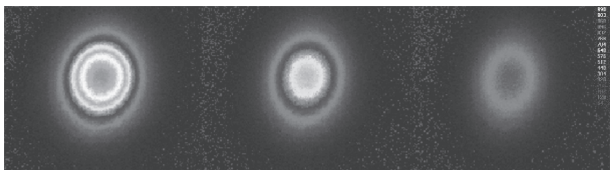

Figure 3. Mode composition of the core of the fibre under study, measured by a beam scanning technique.

Light absorption from the cladding was measured by a cutback technique. At the pump wavelength (0.915 μm), absorption from the cladding was 3.4 dB m^{-1}. The loss due to the fusion splicing of the test fibre to a step-index fibre with a mode field diameter near 10 μm ($\Delta n = 0.002$) did not exceed 0.35 dB. In the case of fundamental mode excitation by light polarised along one of the fibre axes, the polarisation extinction ratio at the output of a 1-m length of the fibre exceeded 23 dB.

4. Small-signal amplifier based on the Yb-doped fibre

The ytterbium-doped fibre was tested in a small-signal amplifier scheme (Fig. 4). As a narrow-band signal source ($\Delta\lambda \sim$ 0.06 nm), we used a fibre-pigtailed semiconductor laser diode. The LD wavelength was stabilised by a low-reflectivity (15% to 20%) fibre Bragg grating located 1 m from the laser diode. The signal wavelength was varied by changing the Bragg grating. The signal power delivered to the active fibre was estimated from the signal power at the free end of a coupler fusion-spliced to the output end of the Bragg grating (Fig. 4), with allowance for the splice loss and the loss in the components of the amplifier. To avoid damage to the signal LD by 0.98-μm luminescence, an isolator was placed before the amplifying part of the scheme.

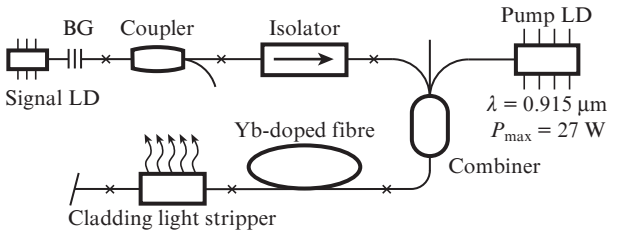

Figure 4. Schematic of the amplifier (BG = Bragg grating).

The signal and pump beams were coupled into the active fibre using a specially designed, fusion-spliced fibre combiner [(2 + 1)× 1 configuration], whose signal fibre had core and cladding diameters of 10 and 80 μm, respectively. The numerical aperture of the signal fibre's core was 0.08. As pump ports, we used 105/125 multimode fibre with NA = 0.22. The power loss of the pump beam, propagating through the cladding, in the pump combiner was 0.8 dB. The power loss of the signal beam, propagating through the core, was 2.9 dB. The pump source used was a commercially available fibre-pigtailed (105/125) multimode LD emitting near 0.915 μm and having a maximum output power of 27 W. The unabsorbed pump light was removed from the system using a specially designed 10/125 fibre cladding light stripper [12]. The stripper was spliced to fibre having the same diameter (10 μm) and core NA, but coated with a high refractive index polymer, which allowed the residual pump light to be removed from the cladding. The output end of this fibre was angle-cleaved at about 8° to suppress signal back reflection. The length of the active fibre maximising the amplification efficiency near 0.976 μm was 45 cm.

5. Results and discussion

Figure 5 shows signal amplification efficiency as a function of the wavelength of propagating light in the saturation regime (input signal power of 50 mW) for the fibre under study. It is seen that the gain has a maximum near 0.977 μm. The corresponding amplification efficiency is 9.7% (Fig. 6). The threshold pump power for cw lasing does not exceed 3 W, which is substantially lower than that in known amplifiers based on cladding-pumped specialty fibres [1–5]. Thus, to obtain a relatively low output power (at a level of 1 W), a minimum pump power (compared to other fibre designs intended for amplification near 0.976 μm) is required in our case.

It is worth noting that the amplification efficiency calculated for the real RIP, with allowance for the measured radial ytterbium profile [with the radius of the doped region taken to be the average of the minimum (x axis) and maximum

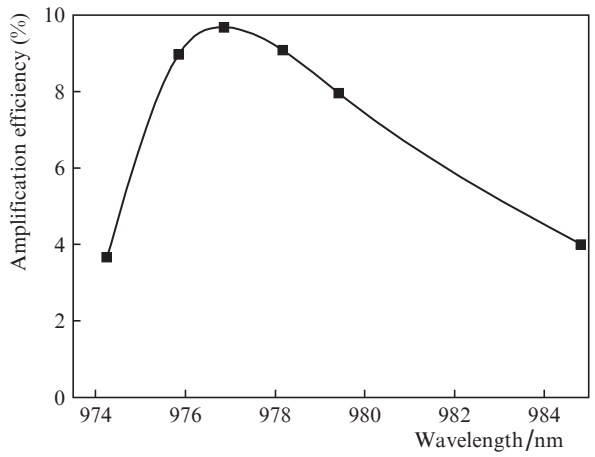

Figure 5. Signal amplification efficiency in the saturation regime at the maximum pump power.

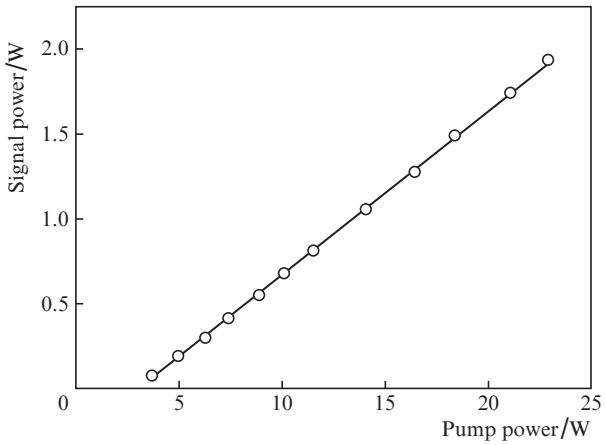

Figure 6. Output signal power (λ = 0.977 μm) as a function of pump power.

(y axis) radii of the doped region] and particular experimental conditions (pump power and input signal power), was 17%. The optimal fibre length was 75 cm (Fig. 7). Note that, according to calculation, the amplification efficiency at an active fibre length of 45 cm is 10.7%, which is close to the value obtained in this study. The discrepancy between the calculated and experimentally determined optimal lengths (with a more rapid rise in luminescence at a wavelength of 1.03 μm observed in experiments) can be accounted for in terms of luminescence 'capture' by cladding modes, which can have an appreciable overlap with the fibre core because of the small diameter of the first reflective cladding. As shown earlier [13], multimode light propagation at a luminescence wavelength leads to a decrease in the optimal length of the active fibre amplifying at wavelengths near 0.976 μm. Additional factors that can be responsible for the reduction in efficiency are core ellipticity and the uneven Yb^{3+} distribution across the fibre (the central part of the core had a higher Yb^{3+} concentration).

To assess the feasibility of using the fibre as a small-signal amplifier, we examined the effect of input signal power on the signal-to-noise ratio at the amplifier output (the ratio of the amplified signal power to the integrated luminescence power near 0.976 μm). The level of luminescence with a maximum near 1.03 μm was left out of consideration owing to the possibility of effective light filtering in this spectral region with

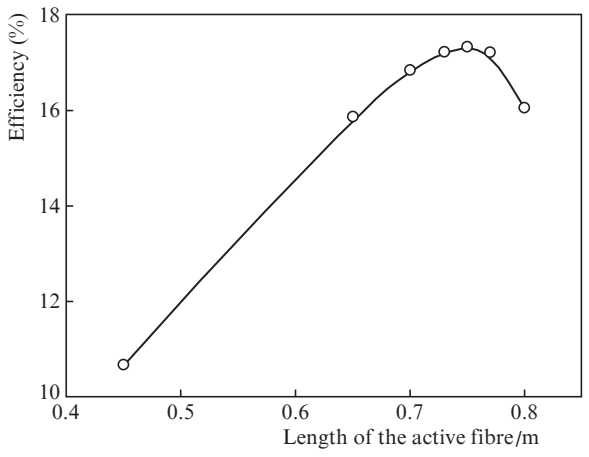

Figure 7. Signal amplification along the length of the active fibre calculated with allowance for the dopant distribution across the fibre and experimental conditions.

the use of commercially available fibre filters. The measurements were performed in the spectral range 0.974–0.985 μm. To ensure identical input signal parameters, the scheme included an input signal attenuator, which allowed the signal power to be varied from 10 μW to 50 mW.

As an example, Fig. 8 shows the added power at a wavelength of 976.9 nm and the generated luminescence power at 0.98 and 1.03 μm as functions of input signal power. The data determine the best signal-to-noise ratio because the input signal wavelength corresponds to the highest gain. Thus, at an input signal power near 1 mW, a signal-to-noise ratio above 20 dB can be achieved, which is quite sufficient for most applications. Figure 9 shows the spectral dependence of the signal-to-noise ratio measured for a narrow-band source at an input signal power of 1 mW. Analysis of gain spectra obtained at an input signal power of 10 μW demonstrated the feasibility of reaching a gain of ~40 dB. Note that, in this case, a large signal-to-noise ratio can be ensured using spectral filters capable of suppressing luminescence at wavelengths differing from the wavelength of the signal being amplified (which is

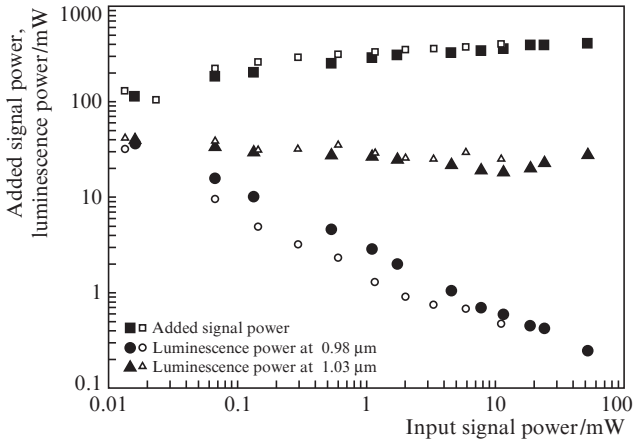

Figure 8. Signal power at the amplifier output and luminescence power near 0.98 and 1.03 μm as functions of input signal power. The input signal was provided by one (976.9 nm, closed symbols) or two (975.8 and 977.3 nm, open symbols) sources, whose wavelengths fell in the peak gain region of the Yb^{3+} ion.

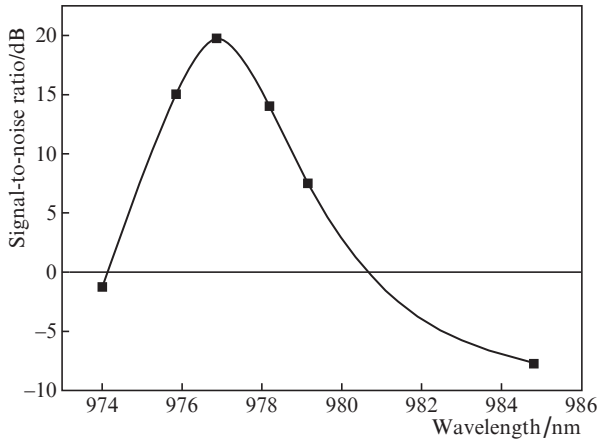

Figure 9. Spectral dependence of the integrated signal-to-noise ratio at an input signal power of 1 mW.

most effective for amplification of a single-frequency or narrow-band signal). Figure 10 shows the spectral dependence of the measured gain coefficient for a small signal of 10-μW power. It follows from these data that the gain exceeds 25 dB in the spectral range 974–980 nm.

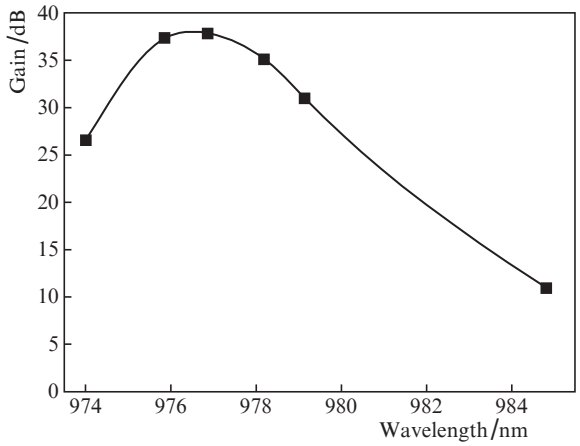

Figure 10. Gain as a function of wavelength for a 10-μW signal.

Note also that the shape of amplified spontaneous luminescence spectra depended on the wavelength of the signal being amplified. We believe that this is due to the inhomogeneous broadening of Yb^{3+} luminescence spectra, as a result of which population inversion elimination and the decrease in luminescence intensity are nonuniform and occur predominantly at the signal wavelength and in its vicinity [4]. The present data lead us to assume that the use of broadband light will allow the 0.98-μm luminescence intensity to be further reduced.

To verify this assumption, we carried out experiments in which we amplified a signal at two wavelengths (one component at 975.8 nm and the other at 977.3 nm) in the region of the maximum in gain. Light amplification at these wavelengths was studied both separately and simultaneously. In both cases, the integrated input signal power was unchanged. In the case of the simultaneous amplification of a 'broadband' signal consisting of two spectral components, their powers were set to be equal to each other. All spectra were measured at fixed positions of the fibres, components of the scheme and spectrum measurement devices and a constant pump power. The results are presented in Fig. 11, together with the luminescence spectrum obtained at the same pump power but with no input signal. It is seen that narrow-band signal amplification leads to significant changes in the luminescence spectrum of the output signal, with a characteristic 'dip' around the signal wavelength. The gain spectrum of the 'broadband' signal contains spectral components analogous to those observed in the case of the independent amplification of each signal, but it is seen in Fig. 11 that there is a considerable 'dip' between the spectral components in the luminescence spectrum. Thus, a broadband input signal spectrum allows the integrated 0.98-μm luminescence power to be reduced. The luminescence spectrum obtained with no input signal corresponds to the maximum luminescence intensity at a given pump power.

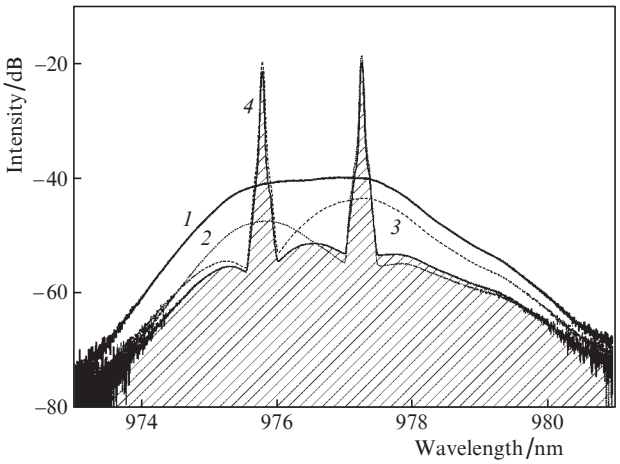

Figure 11. Spectra at the amplifier output: (*1*) luminescence with no input signal; (*2*) signal at $\lambda = 975.8$ nm; (*3*) signal at $\lambda = 977.3$ nm; (*4*) 'broadband' signal consisting of two components at $\lambda = 975.8$ and 977.3 nm. The pump power was 8.9 W and the integrated signal power was 140 μW.

For the amplification of a 'broadband' signal (consisting of two spectral components), we measured the output signal and integrated luminescence intensity near 0.976 and 1.03 μm. Under such conditions, the signal-to-noise ratio for small-signal amplification was almost 4.5 dB better than in the case of narrow-band signal amplification (Fig. 8).

6. Conclusions

We have developed and demonstrated an all-silica active fibre design for light amplification at $\lambda = 0.98$ μm and fabrication of all-fibre cladding-pumped laser and amplifier systems. The main idea of this study is additional doping of the fibre cladding in order to raise the rate of pump absorption from the cladding. The proposed fibre has been tested in an all-fibre small-signal amplifier. The fibre has been demonstrated to have considerable potential for small-signal amplification. The signal-to-noise ratio has been shown to depend on the spectral width of the signal being amplified.

Acknowledgements. This work was supported by the Russian Science Foundation (Grant No. 18-79-00187).

References

1. Boullet J., Zaouter Y., Desmarchelier R., Cazaux M., Salin F., Saby J., Bello-Doua R., Cormier E. *Opt. Express*, **16** (22), 17891 (2008).
2. Röser F., Jauregui C., Limpert J., Tünnermann A. *Opt. Express*, **16** (22), 17310 (2008).
3. Leich M., Jäger M., Grimm S., Hoh D., Jetschke S., Becker M., Bartelt H. *Laser Phys. Lett.*, **11** (4), 045102 (2014).
4. Matniyaz T., Li W., Kalichevsky-Dong M., Hawkins T.W., Parsons J., Gu G., Dong L. *Opt. Lett.*, **44**, 807 (2019).
5. Aleshkina S.S., Likhachev M.E., Lipatov D.S., Medvedkov O.I., Bobkov K.K., Bubnov M.M., Guryanov A.N. *Proc. SPIE*, **9728**, 97281C (2016).
6. Aleshkina S.S. et al. *IEEE Photonics Technol. Lett.*, **30** (1), 127 (2018).
7. Nilsson J., Minelly J.D., Paschotta R., Tropper A.C., Hanna D.C. *Opt. Lett.*, **23**, 355 (1998).
8. Eidam T., Rothhardt J., Stutzki F., Jansen F., Hädrich S., Carstens H., Jauregui C., Limpert J., Tünnermann A. *Opt. Express*, **19** (1), 255 (2011).
9. Koponen J., Laurila M., Hotoleanu M. *Appl. Opt.*, **47** (25), 4522 (2008).
10. Likhachev M., Aleshkina S., Shubin A., Bubnov M., Dianov E., Lipatov D., Guryanov A. *Proc. CLEO/Europe and EQEC 2011* (Munich, 2011) paper CJ_P24.
11. Unger S., Schwuchow A., Jetschke S., Reichel V., Scheffel A., Kirchhof J. *Proc. SPIE*, **6890**, 689016 (2008).
12. Aleshkina S.S., Kochergina T.A., Bobkov K.K., Kotov L.V., Bubnov M.M., Park J., Likhachev M.E. *Proc. CLEO 2016* (San Jose, USA, 2016) paper JTu5A.106.
13. Aleshkina S.S., Bardina T.L., Lipatov D.S., Bobkov K.K., Bubnov M.M., Gur'yanov A.N., Likhachev M.E. *Quantum Electron.*, **47** (12), 1109 (2017) [*Kvantovaya Elektron.*, **47** (12), 1109 (2017)].